The Structure and Vorticity Budget of an Early Summer Monsoon Trough (Mei-Yu) over Southeastern China and Japan

TAI-JEN GEORGE CHEN[1] AND CHIH-PEI CHANG

Department of Meteorology, Naval Postgraduate School, Monterey, CA 93940

(Manuscript received 5 July 1979, in final form 28 February 1980)

ABSTRACT

One of the most persistant rain-making events over East Asia is the development of an early summer monsoon trough (Mei-Yu) which extends from southeastern China to southern Japan. This work studies the structure and vorticity budget of a Mei-Yu system for the period 10–15 June 1975.

Subjectively analyzed grid-point data are time composited with respect to the trough axis along three cross sections over southeastern China (western section), southern East China Sea (central section) and southern Japan (eastern section), respectively, during the mature and decaying stages of the trough. The results indicate that the structure of the eastern and central sections resembles a typical midlatitude baroclinic front with strong vertical tilt toward an upper level cold core and a strong horizontal temperature gradient. On the other hand, the western section resembles a semitropical disturbance with an equivalent barotropic, warm core structure, a weak horizontal temperature gradient, and a rather strong horizontal wind shear in the lower troposphere.

Cumulus convection activity south of the 850 mb trough is significant in all three sections and contributes substantially to the thermally direct secondary circulation, but the large-scale organizing mechanism differs from one section to another. In the eastern and central sections it is mainly due to differential vorticity advection while in the western section it is due to Ekman pumping (CISK). The generation of cyclonic vorticity is counteracted by cumulus damping in the eastern section and by boundary layer friction in the mountainous western section.

1. Introduction

During the pre- and early summer period of mid-May to mid-June, a rain-producing phenomenon dominates the weather over the coastal regions of East Asia including Japan and southeastern China. This period represents the local rainfall maximum each year outside of the summer typhoon season. The rainfall during this period is called "Mei-Yu" (plum rain) in China and "Baiu" in Japan. It may be continuous or intermittent for several days to a few weeks and includes frequent rainshowers and thunderstorms, with rainfall rate of up to a few hundred millimeters per day. Synoptically this rainfall is associated with the repeated occurrence of a front which develops in the midlatitudes and slowly moves southeastward to establish a quasi-stationary position extending from southern Japan to southern China. The front's position coincides with the early summer monsoon trough in East Asia and its existence may be viewed as a manifestation of the trough. The beginning of the rainy season also signifies the onset of the northern summer monsoon in this part of the world.

The Severe Rainstorms Research Project of the Japan Meteorological Agency has carried out several experiments in the Kyusku district and its adjacent oceanic areas during the Baiu seasons of 1968–72 to study the heavy rainfall. One of the main findings from the experiments is that the front is characterized by a smaller horizontal temperature gradient than that in a typical polar front but is accompanied by an ageostrophic low-level jet stream (e.g., Matsumoto *et al.*, 1971). The heavy rainfall was found to be associated with this jet which is presumably due to the downward transport of horizontal momentum by cumulus convection (Matsumoto, 1972; Akiyama, 1973). Mesoscale convective systems were observed to be imbedded in the intermediate-scale cyclones or weak depressions in the Baiu front and were responsible for the intense rainfalls (Ninomiya and Akiyama, 1971, 1972; Akiyama, 1974).

There is relatively little work reported in the open literature pertaining to the study of the Mei-Yu front over southeastern China and its vicinity. Recently Chen and Tsay (1977, 1978) carried out a detailed synoptic analysis of a Mei-Yu system during 10–15 June 1975 and provided, for the first time, a data base of relatively high resolution for a Mei-Yu system. Since the eastern part of the Mei-Yu front is over

[1] Permanent affiliation: Department of Atmospheric Sciences, National Taiwan University, Taipei 107 Taiwan, R.O.C.

0027-0644/80/070942-12$07.00

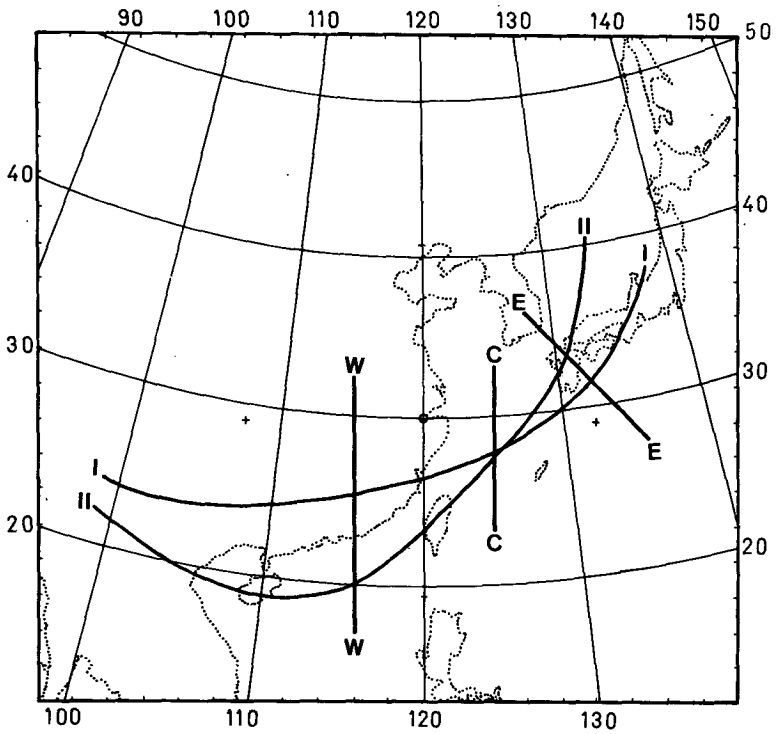

FIG. 1. Mean positions of 850 mb Mei-Yu trough during stages I and II and the cross sections W, C and E.

central and southern Japan and extends as far north as ~40°N, while the western part of the front penetrates to the northern part of the South China Sea south of 20°N, the front may be viewed as a combined midlatitude and tropical system. This property is especially interesting in view of the role of the Mei-Yu systems in the northern summer monsoon of East Asia. The purpose of this paper is to compare the eastern, western and central segments of a Mei-Yu front in terms of the cross-sectional structure and vorticity budgets using Chen and Tsay's (1977) data set. Although the cross-section analysis does not allow an explicit accounting of the mesoscale disturbances imbedded in the front, we hope that the present study will be a first step toward revealing the basic characteristics of the mean states of the different segments and that it will provide a basis for understanding the similarities and differences between the different segments which form the combined midlatitude-tropical system.

2. Data and method of analysis

The subjective analysis of the 10–15 June 1975 case by Chen and Tsay (1977) was done twice daily at all mandatory levels over the area between 10–55°N and 85–150°E. The data were tabulated at 240 km grid intervals after a 25-point smoothing (Bosart, 1970). They also computed the kinematic vertical velocity and vorticity budget terms at the individual times using centered finite differences for all space and time derivatives. The kinematic vertical velocity was adjusted according to the smoothed-terrain Ekman pumping value at 850 mb and adiabatic value at 100 mb. The vorticity equation used was

$$\frac{\partial \eta}{\partial t} = -\mathbf{V}\cdot\nabla\eta - \eta\cdot\nabla\mathbf{V} - \omega\frac{\partial \eta}{\partial p} - \mathbf{k}\cdot\nabla\omega\times\frac{\partial \mathbf{V}}{\partial p} + F,$$

where all the notations are conventional. Each term was computed directly, except the friction term (F) which was the residual necessary for balancing the equation.

In addition to Chen and Tsay's data, high-resolution Defense Meteorological Satellite Program imageries are used to subjectively estimate the total and the cumulonimbus (Cb) cloud covers within each 1° longitude-latitude square. These estimates are then averaged over each 2° × 2° grid. The Cb clouds are determined by the brightness and degree of organization in the visible imageries and by the whiteness (indicating cold cloud top) in the infrared imageries.

Three cross sections (W, C and E) are chosen to depict the structure in the western, central and eastern segments, respectively, of the Mei-Yu system (Fig. 1). Section W is oriented north-south

over southeastern China and is approximately perpendicular to the 850 mb Mei-Yu trough (defined by the minimum geopotential line on the isobaric surface). The trough in this area moves slowly southward for the entire period of study. Section C, also oriented north-south, lies over the East China Sea and intersects the nearly stationary part of the 850 mb trough at a 60° angle. Section E, which is oriented northwest-southeast across Korea and southern Japan, is similar to section W, roughly perpendicular to the 850 mb trough. This trough moves back and forth in a northwest-southeast direction over this area during the period of study.

In order to reduce the amount of data for easy discussion, the 12 h data are composited within each of two stages which are defined by the intensity of the cyclonic vorticity associated with the 850 mb Mei-Yu trough over southeastern China (Section W). Fig. 2a shows the time cross section of relative vorticity and the trough position (dashed line) at 850 mb for section W. Based on this figure, the entire period is divided into stages I and II, which cover the periods 0000 GMT 10 June to 1200 GMT 12 June and 0000 GMT 13 June to 1200 GMT 15 June, respectively. Each stage contains data of six synoptic times at 12 h intervals. Stage I represents the mature stage during which the maximum cyclonic vorticity associated with the trough in Section W is approximately conserved. Stage II represents the decaying stage within which the averaged maximum cyclonic vorticity in section W decreases more than 50% from that of stage I. Figs. 2b and 2c show the relative vorticity and trough position for sections C and E, respectively. Notice that the two stages defined above do not necessarily imply similar intensity changes as that in section W. In section E the averaged maximum vorticity decreases by ~20% from stages I to II, but in section C it increases by more than 30%. It will be shown later, however, that stage II in general represents a decaying stage for all three sections as far as the intensities of the height-trough, temperature gradient and convective activity are concerned.

The compositing is done by time-averaging data, within each stage, that are categorized with respect to the 850 mb trough for all mandatory levels between 850 and 400 mb for all three sections. No surface data are used as the height of terrain varies between sea level and 1.1 km.

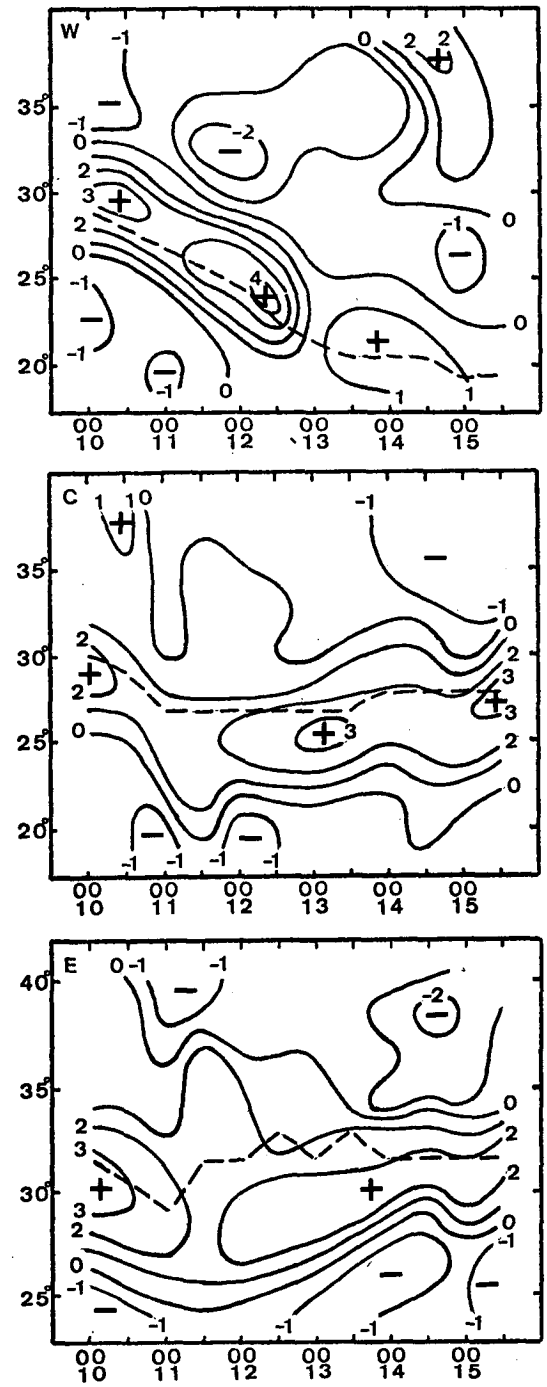

FIG. 2. Time-latitude cross sections of relative vorticity (10^{-5} s^{-1}) at 850 mb in (a) section W, (b) section C and (c) section E.

3. Sectional structure of the Mei-Yu trough

a. Mean position and movements of the 850 mb trough

As shown in Fig. 1, the 850 trough moves in somewhat different manners in the three sections. In section W the trough moves southward at an averaged speed of 9 km h^{-1} during stage I and slows down to 6 km h^{-1} during stage II. The mean positions of the trough are located near 26 and 20°N in stages I and II, respectively. In section C the trough is nearly stagnant at about 28°N. In section E it migrates between 28–35°N with a mean position shifting from 38°N northwestward to 32°N from stages I to II.

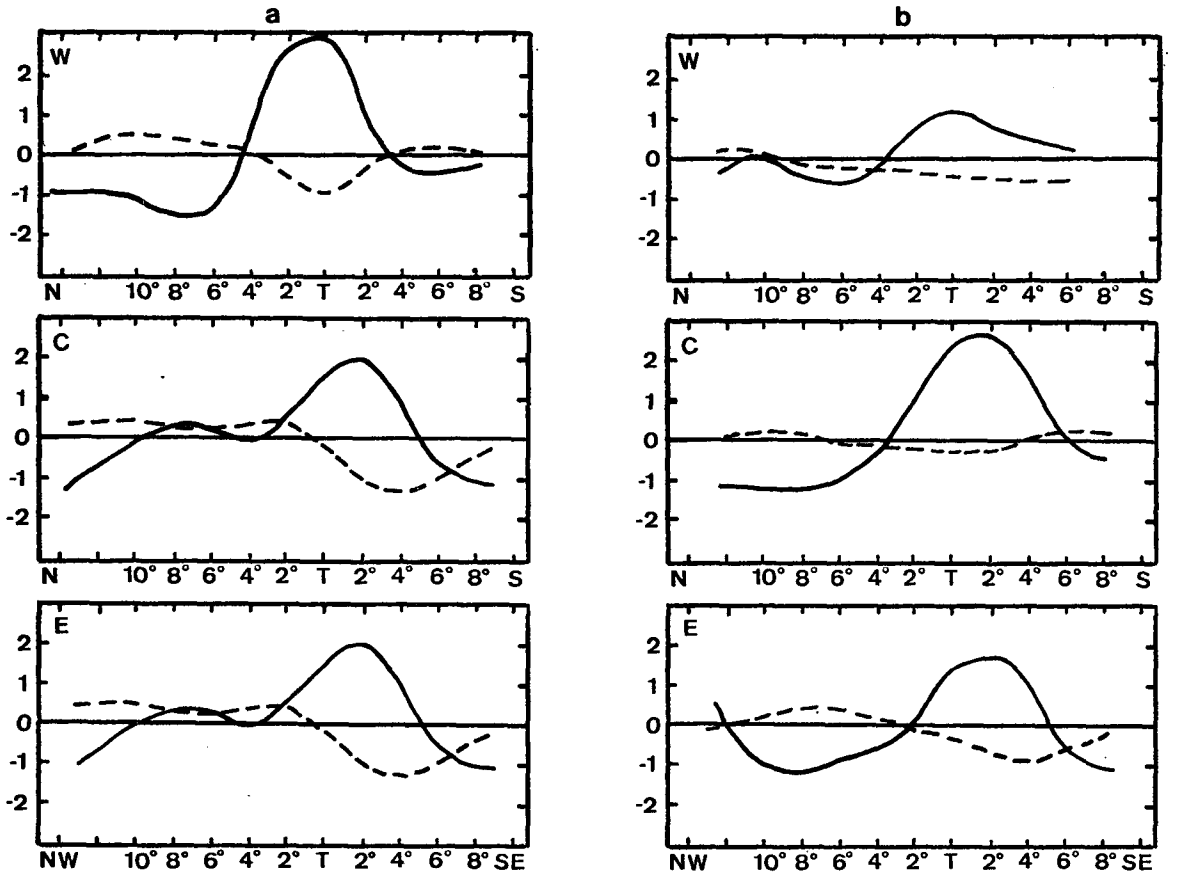

FIG. 3. Distribution of relative vorticity (solid) and divergence (dashed) at 850 mb in sections W, C and E during (a) stage I and (b) stage II. Units are 10^{-5} s^{-1}. The abscissa indicates distance in degrees latitude from the trough (T).

b. Geopotential height

The distribution of geopotential height in the three sections is described here but their diagrams are not shown explicitly. Instead, the vertical trough lines are shown in the diagrams of all other cross sections. In section W the trough is quite shallow, being well defined only at 850 and 700 mb in stage I with essentially no vertical tilt. It becomes ill defined at these two levels in stage II. Above 700 mb it is totally indiscernible in both stages.

The trough in section C, on the other hand, is well defined at all levels up to 400 mb (the highest level analyzed) and tilts significantly northward in stage I. The geopotential gradient weakens only slightly in stage II.

Similar to section C, the trough in section E during stage I is also well defined and tilted at all levels up to 400 mb except that the tilt is somewhat smaller. It weakens slightly in stage II with no change in the tilt. The moderate tilt resembles that of a typical frontal cyclone in its occluded stage.

c. Relative vorticity

Time cross sections of relative vorticity and trough position at 850 mb (Fig. 2) indicate that the Mei-Yu trough is within a zone of cyclonic vorticity. The maximum of this vorticity coincides with the trough in section W and is to the immediate south or southeast of the trough in sections C and E. It is clear that from stages I to II the width of the cyclonic vorticity zone broadens in section W, remains nearly unchanged in section C and narrows in section E.

The 850 mb relative vorticity in both stages in all three sections is shown in Fig. 3. Although the relative position of the vorticity maximum varies between the three sections, their magnitudes during stage I are comparable, all of the order of 2–3 $\times$ 10^{-5} s^{-1}. From stages I to II this magnitude decreases by 60% in section W, 20% in section E and increases by 30% in section C, as may be inferred from Fig. 2.

At 700 mb (not shown) the vorticity maximum is situated 2° latitude north of the 850 mb trough in section W and directly over the 850 mb trough in sections C and E during both stages. The magnitude in stage I is comparable to that at 850 mb in sections C and E but is smaller in section W. From Stages I to II this magnitude is reduced by 70, 30 and 20% in sections W, C and E, respectively.

In all three sections the cyclonic vorticity is

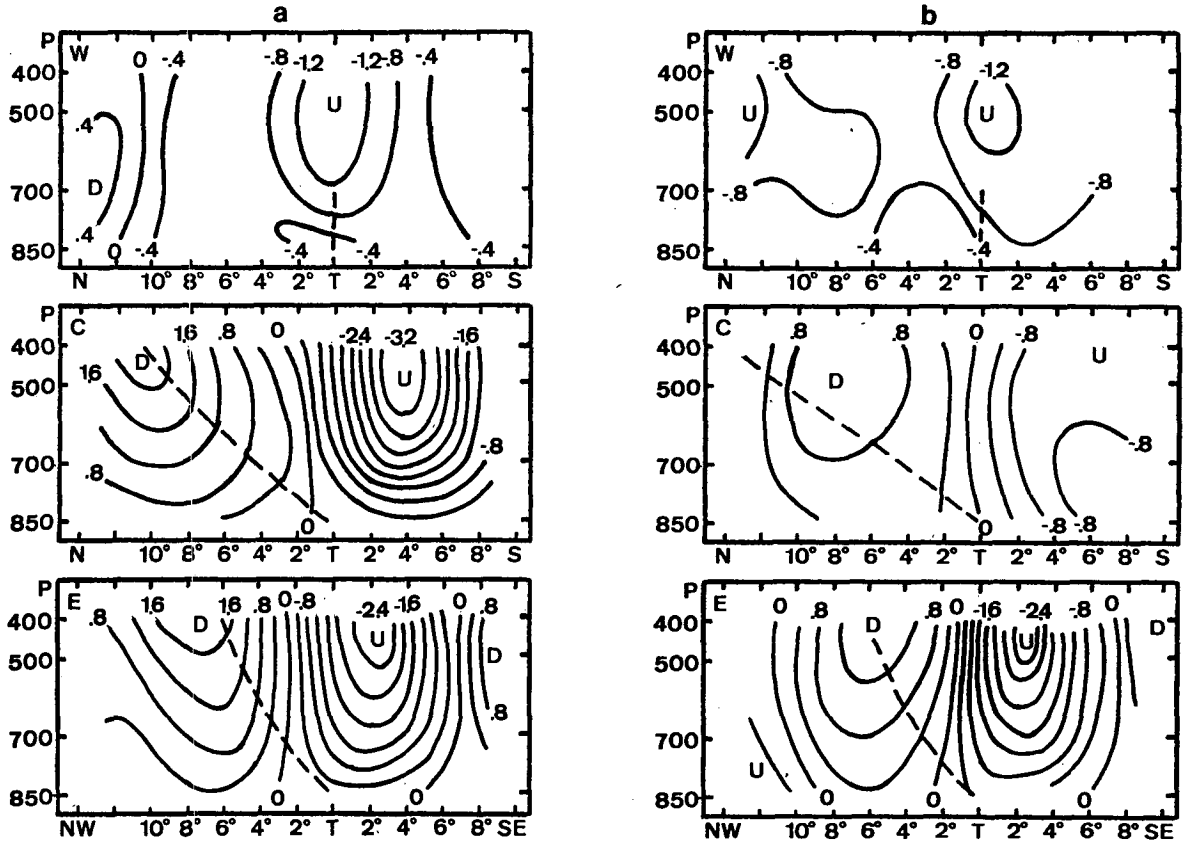

FIG. 4. Vertical cross sections of pressure velocity (μb s^{-1}) in sections W, C and E during (a) stage I and (b) stage II. Dashed lines indicate the trough axes. The abscissa is distance in degrees latitude.

mainly due to the shear, across the Mei-Yu trough, of the wind component parallel to the trough. In stage I this shear at 850 mb is about twice as large in section W as in sections C and E. In stage II it decreases remarkably in section W by 80% at 850 mb and 95% at 700 mb. However, it decreases by only 25% at 850 mb and 55% at 700 mb in section C and remains practically unchanged at both levels in section E.

d. Horizontal divergence

Horizontal divergence at 850 mb during both stages is also shown in Fig. 3. The error of composited divergence is estimated to be $<10^{-6}$ s^{-1}. The convergence maximum coincides with the vorticity maximum and the 850 mb trough in section W. However, the vorticity maximum is found to lie between the trough and the convergence maximum in sections C and E. The magnitude of convergence is comparable among the three sections during stage I. In stage II it is reduced substantially in sections W and C but only slightly in section E. At 700 mb (not shown), the distribution is very similar to that at 850 mb except the magnitude is slightly smaller.

e. Vertical velocity

Vertical cross sections of the pressure velocity (ω) in both stages are shown in Fig. 4. In stage I the upward motion reaches maximum at 500 mb in all three sections. It is located over the 850 mb trough in section W, 4° latitude south of the trough in section C and 3° latitude southeast of the trough in section E. On the north side of the trough downward motion prevails with a maximum at 400 mb in sections C and E, and at 700 mb in section W. This well-organized vertical velocity couplet is indicative of the existence of a well-developed secondary circulation normal to the trough. In stage II the circulation becomes substantially less vigorous in sections W and C, but it maintains its intensity in section E.

f. Temperature

Fig. 5 shows the vertical cross sections of the deviation of temperature (T') from the cross-sectional mean at each level. Here the mean value is the average over a distance of 2500 km from 1000 km south of the trough to 1500 km north of it. This distance is the approximate length scale, along the

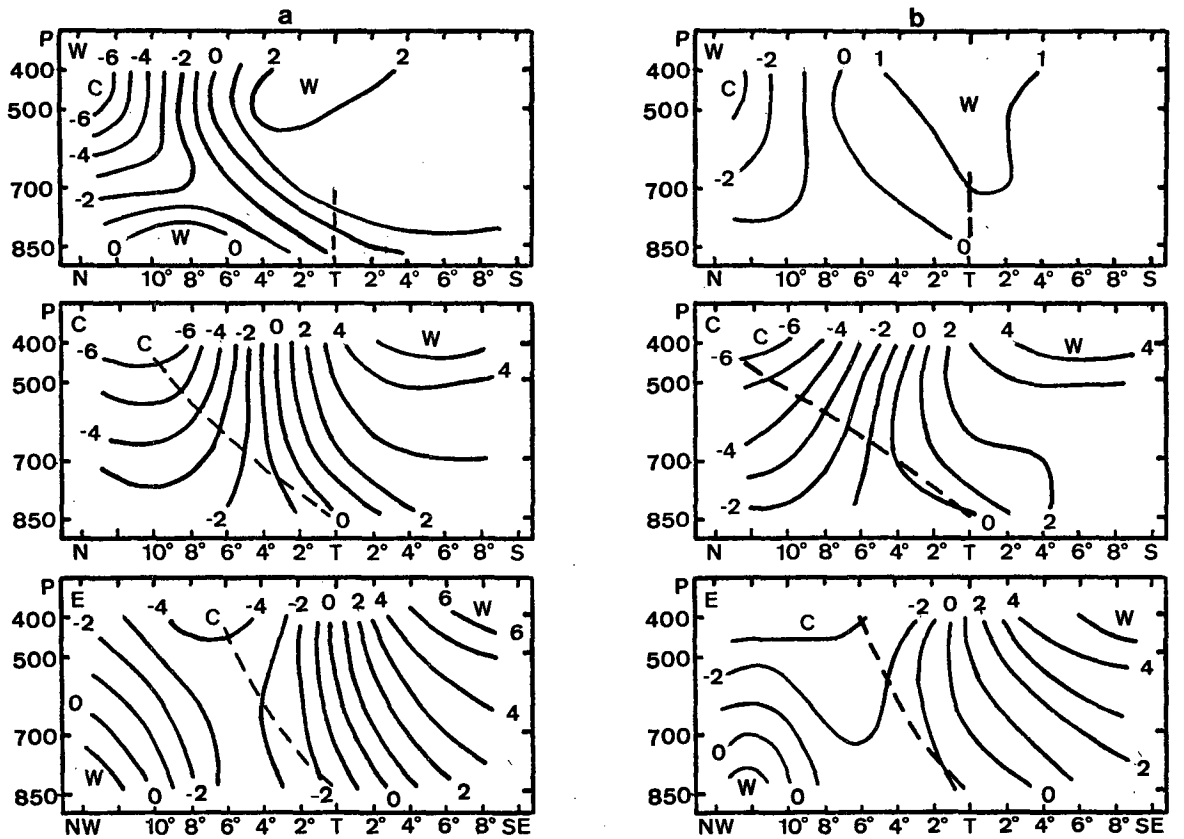

FIG. 5. As in Fig. 4 except for T' (°C).

normal direction of the Mei-Yu system, of the lower tropospheric relative vorticity.

The maximum T' for all cases are found in the upper-middle troposphere near 400 mb. In section W the warmest air is found in the middle troposphere right above the 850 mb trough. This is hydrostatically consistent with the shallowness of the trough in this section. On the other hand, the mid-tropospheric warm air is south of the 850 mb trough in sections C and E. Compared to the vertical velocity distribution (Fig. 4), it is evident that the secondary circulation is thermally direct with warm air rising and cold air sinking. This implies a baroclinic energy conversion which appears to decrease significantly from stages I to II in sectioins W and C where the horizontal gradients of both ω and T' weaken markedly. This conversion remains about the same, however, during the two stages in section E.

g. Mixing ratio

Vertical cross sections of the deviation of mixing ratio (q') in both stages I and II are quite similar. Only those for stage I are shown in Fig. 6. It is seen that the moist air in sections W and C domes upward in the immediate vicinity to the south of the trough and has a northward extension in the mid-troposphere. In section W, the maximum positive q' at all levels coincides with the 850 mb trough except at 850 mb where it is 2° latitude south of the trough. In sections C and E, however, it is located 2–5° latitude south and 4–7° latitude southeast of the trough, respectively.

The upward extension of the moist center into the mid-troposphere correlates positively with the upward vetical velocity and temperature. This may indicate the importance of the vertical moisture transport and the possibility that the warm center in the middle-upper troposphere is largely due to warming by cumulus convection. These points will be reaffirmed by examining the distribution of the satellite cloud data in the next subsection.

h. Satellite cloud cover

The maximum total cloud cover is confined to a rather narrow, elongated band nearly parallel to the 850 mb trough in the warm side (not shown). Fig. 7 shows the distribution in the three cross sections. The maximum cloud band is ~2° latitude from the trough in section W and 4–6° from the trough in sections C and E. During stage I more than half of the total cloud cover within this band is due to Cb activity, which decreases rapidly away from the band

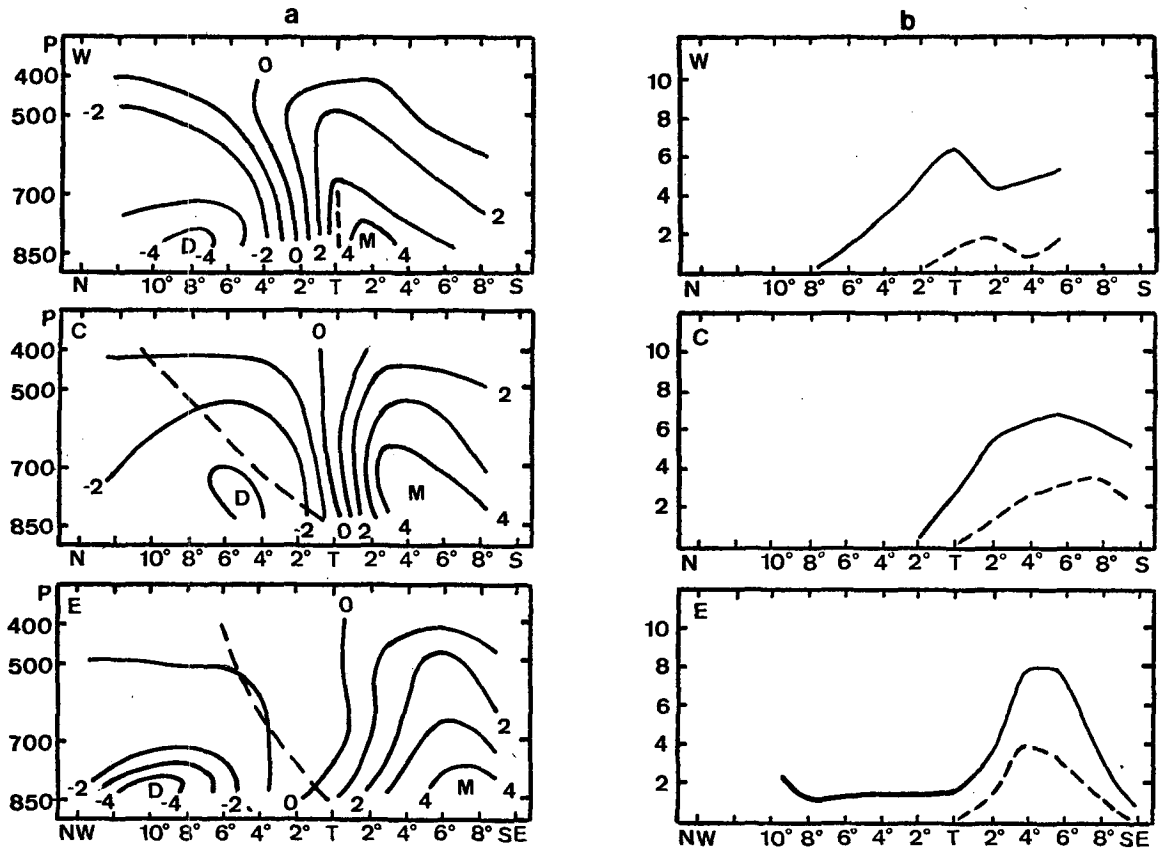

FIG. 6. As in Fig. 4 except for q' (g kg^{-1}).

so that practically no Cb activity is observed in the trough itself. This well-organized band of convection is consistent with the large-scale convergence below 500 mb and the associated upward motion and is indicative of the importance of synoptic-scale control of the convection.

Over and to the north of the 850 mb trough the cloud cover tends to decrease eastward from sections W to E. This is consistent with an examination of the velocity field (not shown) which reveals that during both stages the low-level southwesterly warm and moist flow reaches and even penetrates the trough in section W while it stops short of the trough in the other sections. However, from stages I to II the Cb activity decreases most drastically in section W (by ~70%) whereas it decreases only moderately (by ~20–30%) in sections C and E.

4. Vorticity budgets

Section C is excluded from the composite budget study because it extends over a mainly oceanic area where the data network is not adequate for vorticity budget calculations. Figs. 8 and 9 show the horizontal advection, divergence generation and residual terms for both stages, respectively. All other terms are about one order smaller than the last two terms. The smallness of the local tendency term justifies the compositing of data within each stage. The composited values for all terms represent the individual time values fairly well.

a. Western section

Negative horizontal vorticity advection is found on both sides of the trough at 850 and 700 mb in stage I and reaches a maximum 2–3° latitude south and 4–5° latitude north of the trough. Thus this term does not significantly induce any north-south movement of the trough. In stage II somewhat smaller negative advection remains south of the trough while slightly positive advection is found to the north of the 850 mb trough, suggesting that vorticity advection tends to push the trough northward. The fact that the trough moves southward through both stages implies that the horizontal advection is being overcome by other processes.

Cyclonic vorticity generation due to horizontal convergence prevails in the vicinity of the trough in the lower troposphere and reaches a maximum at 850 mb in stage I. During stage II the generation becomes smaller and is confined ~850 mb in and to

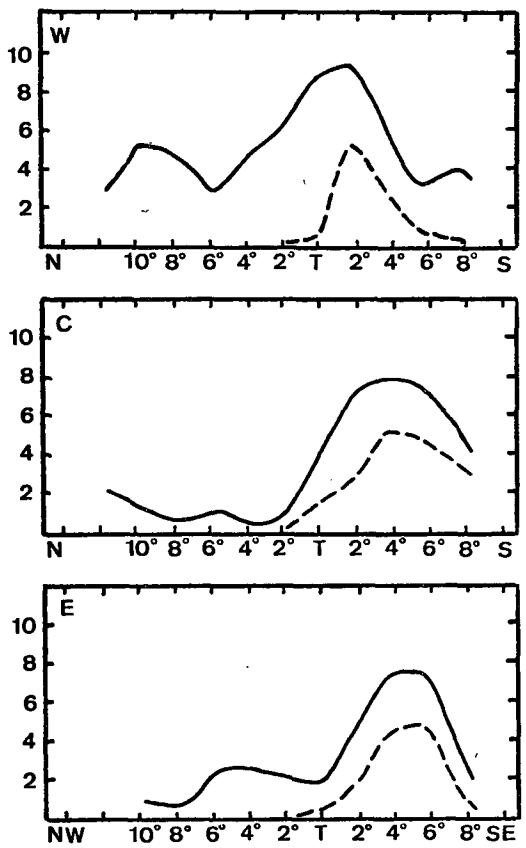

FIG. 7. As in Fig. 3 except for total (solid) and cumulonimbus (dashed) cloud covers. Units are tenths.

the south of the trough, but it is the only positive term in the trough. Thus it is the only process that maintains the intensity of the Mei-Yu trough.

In stage I the residual and divergence terms are comparable in magnitude but with different patterns. The former is negative in and to the north of the trough and positive south of the trough, whereas the latter is positive across the trough. It is seen that the magnitude of the residual term is maximum at 850 mb. In stage II, the negative residual decreases in magnitude but spreads to the south of the trough at 850 mb.

b. Eastern section

Positive vorticity advection over the 850 mb trough increases from 850 to 500 mb during both stages. A negative center of the horizontal advection term in the lower troposphere is found ~4–6° latitude to the warm side of the trough, preventing the trough from moving southeastward.

The generation of cyclonic vorticity by horizontal convergence prevails over and to the southeast of the trough at all levels and reaches a maximum 2–4° latitude to the southeast of the trough in the lower troposphere during both stages. The maximum generation term is found to coincide with cyclonic vorticity maximum at 850 mb.

Negative residual term prevails over and to the southeast of the trough and becomes maximum in the lower troposphere 2–4° latitude to the southeast of the trough in both stages.

5. Discussion

The most apparent difference between the western and eastern sections of the Mei-Yu trough is in the vertical structure. In the western section the trough has practically no vertical tilt and is confined to a shallow layer in the lower troposphere, capped hydrostatically by a warm core in the mid-troposphere. This structure resembles that of many equivalent barotropic, warm-core tropical disturbances (Wallace, 1971). On the other hand, the trough in the central and eastern sections tilt strongly north and northwestward into a cold center near 400 mb, indicating a deep, cold-core baroclinic system which is typical of midlatitudes.

The horizontal temperature gradient near the surface across the Mei-Yu front (Fig. 5) is much weaker in the western section than in the central and eastern sections. (This remains true if the virtual temperature gradient is considered.) However, during the mature stage the cross-trough shear of the wind component parallel to the front is stronger in the western section. This again indicates that the western section is somewhat similar to tropical disturbances in contrast to the midlatitude, strongly baroclinic nature of the other sections. In fact, the weak temperature gradient and strong horizontal wind shear during the mature stage plus the equivalent barotropic vertical structure make the western section look more like an Intertropical Convergence Zone than a typical midlatitude front.

In all three sections the secondary circulation normal to the trough is thermally direct so that available potential energy is converted into kinetic energy locally. The temperature, moisture and cumulus convection distributions correlate very well, indicating that this available potential energy may be generated by latent heat release in the Cb convection area in addition to the normal mid-latitude baroclinic process. Moreover, the change of the degree of convective activity from the mature stage to the decay stage agrees quite well with the change of the intensity of the secondary circulation in each section. Both weaken substantially in the western section, moderately in the central section and remain almost steady in the eastern section.

Although significant cumulus convection is present in all three sections, the roles of large-scale mechanisms responsible for organizing the convection appear to vary. In the western section the low-

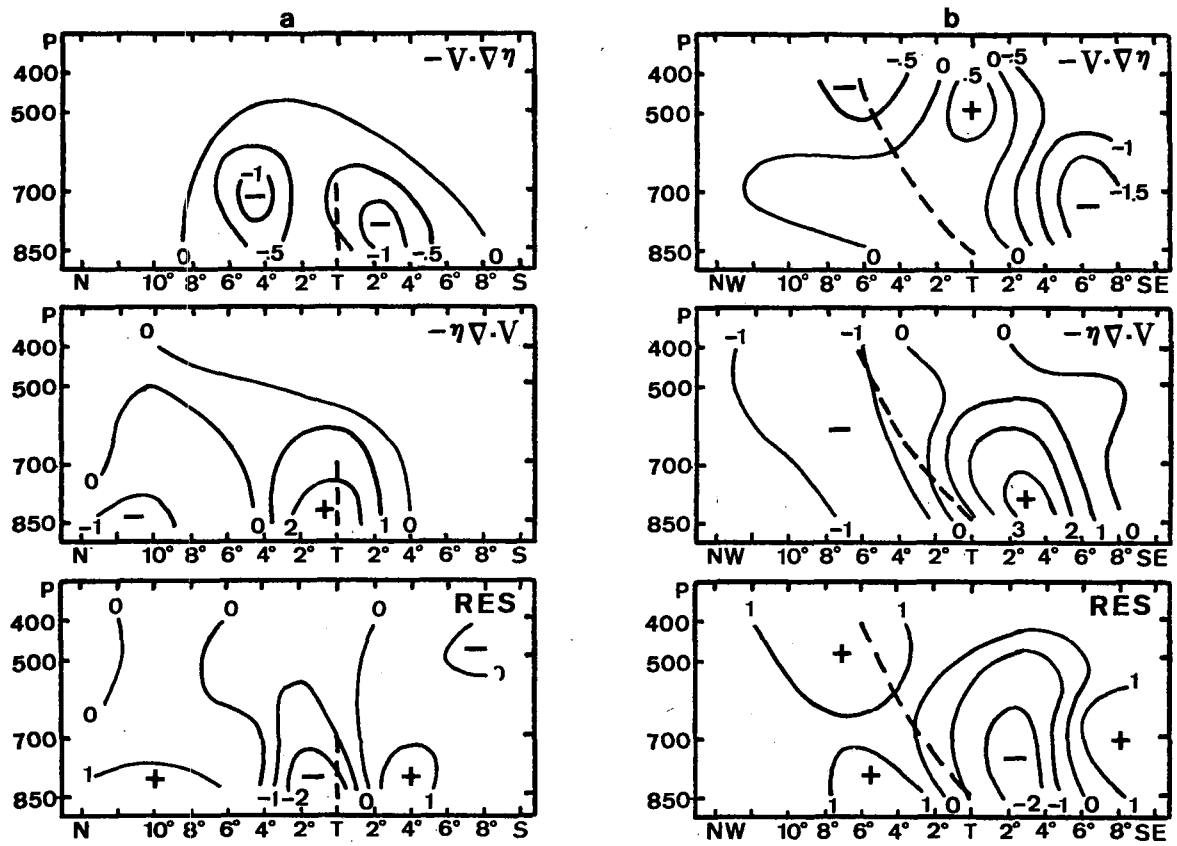

FIG. 8. Vertical cross sections of horizontal vorticity advection, divergence and residual terms during stage I in (a) section W and (b) section E. Units are 10^{-5} s^{-1} (12 h)$^{-1}$. Dashed lines indicate the trough axes. The abscissa is distance in degree latitude.

level vorticity maximum approximately coincides with the low-level convergence center. This suggests that the vertical motion and therefore the cumulus convection may be largely due to Ekman pumping, thus resembling the conditional instability of the second kind (CISK) process. On the other hand, a significant phase difference between the low-level vorticity and convergence is found in the central and eastern sections, indicating that the vertical motion is mostly produced by differential vorticity advection. CISK may still play some role as the vorticity and convergence are slightly positively correlated.

The generation of cyclonic vorticity by horizontal convergence is of primary importance at lower levels. The generation reaches a maximum in or on the warm side of the trough and, even though being partially offset by the residual term, it tends to counteract the retrogression effect of the horizontal advection thereby keeping the trough quasi-stationary.

The residual term in general is negatively correlated with the generation term and represents the damping of vorticity. Several processes may be responsible for this damping. Comparison of the Cb cloud distribution (Fig. 7) and the residual term (Figs. 8, 9) indicates that in the eastern section the maximum damping of the cyclonic vorticity is almost in phase with the area of maximum convection. It therefore seems reasonable to identify the vertical transport by cumulus convection as the damping mechanism in this region. This is similar to the result found by Chen and Bosart (1979) for a composite extratropical cyclone and by numerous others for tropical disturbances (e.g., Reed and Johnson, 1974). However, in the western section the maximum damping of cyclonic vorticity is north of the trough in the cloud-free area where the cyclonic vorticity is also maximum. South of the trough the residual term is positive and acts to dissipate the anticyclonic vorticity at 850 mb. In contrast to the eastern section where the magnitude of the damping term is substantial throughout the lower and middle troposphere, in the western section it is confined to a shallow layer adjacent to the 850 mb.

Fig. 10 shows the smoothed topography in these sections. From this figure and the observed Ekman relationship of the residual term counteracting the divergence term at 850 mb, it is obvious that the mountainous region in southern China, extending to the 850 mb level, exerts a boundary-layer friction effect on the lower tropospheric flow. Thus the damping in the western section ap-

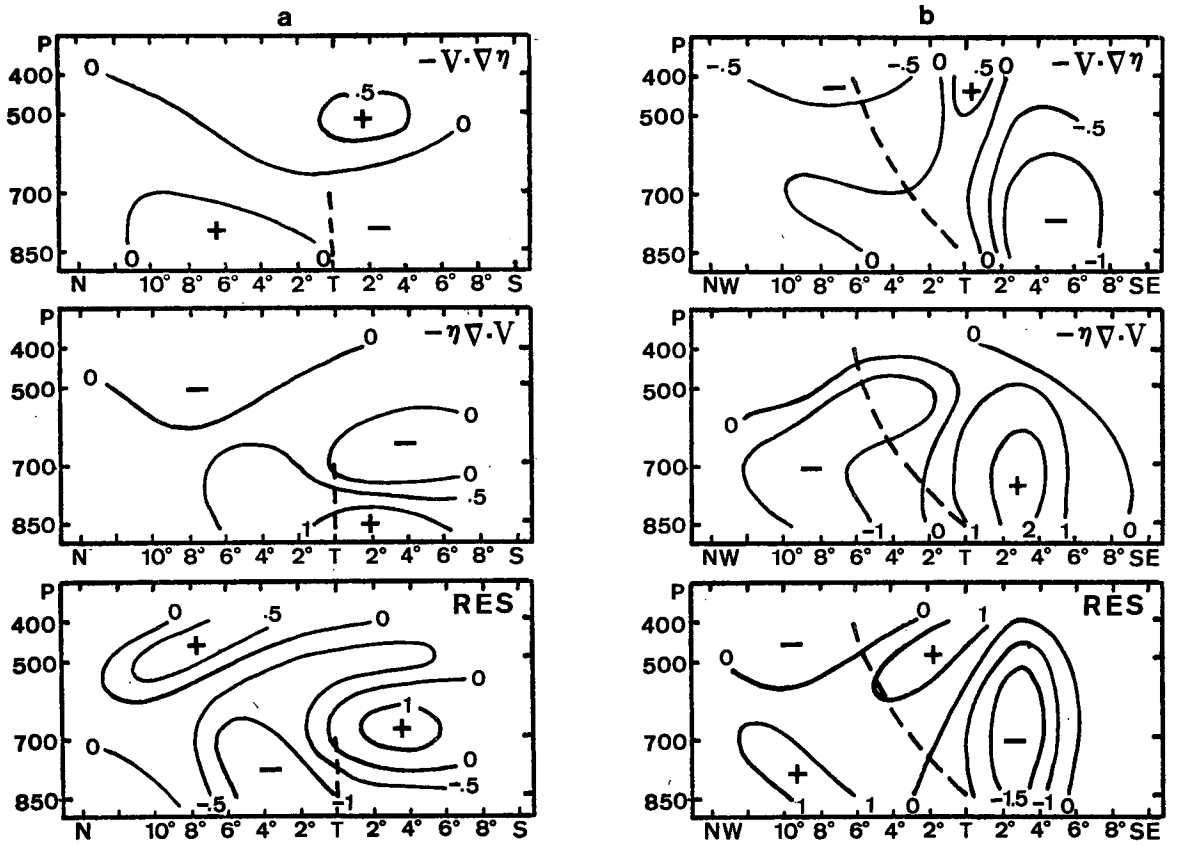

FIG. 9. As in Fig. 8 except for stage II.

parently is more due to the topography than the cumulus convection. The importance of CISK during the mature stage in the western section is consistent with the relative importance of surface friction.

From stages I–II the western section of the low-level trough moves southward off the southern China coast and over the northern part of the South China Sea. The weak horizontal temperature gradient is further reduced throughout the troposphere indicating a decrease in the local baroclinicity. Apparently, this represents a change in the large-scale environment which is sufficient to weaken the trough. This means that the existence of the CISK process depends on the large-scale forcing (frontogenesis) and cannot by itself maintain the trough. The eastern section of the trough moves back and forth over approximately the same area in the two stages and does not experience a significant change in the large-scale flow condition. The cumulus damping and latent heat forcing are proportional to each other resulting in no significant net dissipation of the trough intensity.

6. Summary

This paper studies the structure and vorticity budget of the early summer monsoon trough (Mei-Yu) over subtropical East Asia for the period 10–15 June 1975. Analyzed grid-point data based on the dense upper air station network over southeastern China and Japan are used to construct the cross-sectional structure of the trough along three sections. The trough is manifested at the 850 mb by a quasi-stationary front which moves slowly southward in the western section near the southern China coast, remains nearly stagnant in the central section over the East China Sea between Taiwan and Japan, and fluctuates back and forth in the northwest-southeast direction within a narrow distance over southern Japan. The period of study is separated into two stages, each with six 12 h time intervals, which represent the mature and decay stages of the trough. Within each stage all data in the three sections are time-composited with respect to the trough axis. The main results are as follows:

1) The central and eastern sections of the Mei-Yu trough have a structure resembling a typical mid-latitude baroclinic front with a strong north and northwestward tilt in the vertical toward a middle tropospheric cold core. The horizontal temperature gradient across the trough is strong throughout the troposphere. Significant cumulus convection prevails immediately south or southeast of the 850 mb

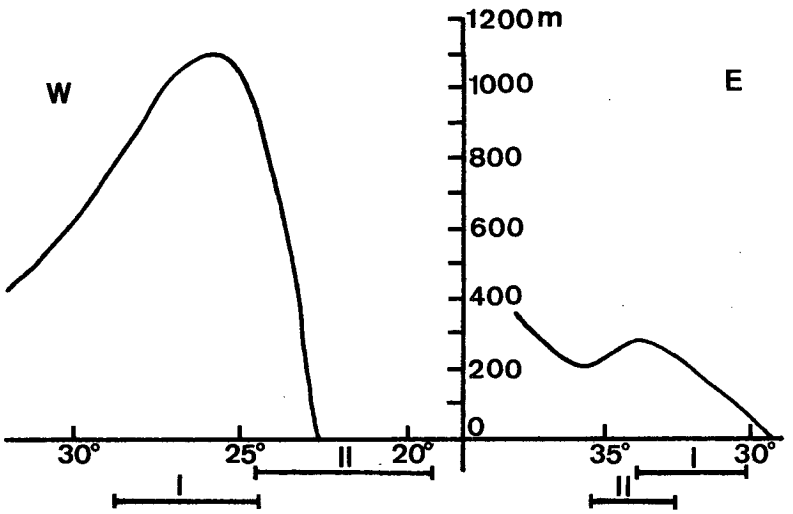

FIG. 10. Smoothed topography in the western and eastern sections. The abscissa is latitude in degrees. The ranges of movement of the 850 mb trough in stages I and II are shown.

trough and apparently contributes substantially to the heating of the middle troposphere which, in addition to the normal midlatitude baroclinic processes, is important in maintaining a thermally direct secondary circulation normal to the trough. However, the low-level vorticity and convergence distribution suggests that CISK plays a small role compared to differential vorticity advection.

2) The western section, which is in lower latitudes and subject to a stronger influence of the moist southwest monsoon flow, exhibits several features that are less common in midlatitude fronts while more typical in tropical systems such as the ITCZ. The trough is confined to a shallow layer in the lower troposphere with almost no vertical tilt and it is capped by a mid-tropospheric warm core resembling an equivalent barotropic system. The horizontal temperature gradient is much weaker than in the eastern section but during the mature stage the horizontal wind shear across the trough is stronger. There is also intense cumulus convection and a thermally direct secondary circulation and both appear to be induced by a CISK process.

3) The generation of cyclonic vorticity by horizontal convergence in both eastern and western sections is offset by strong damping processes. In the eastern section the damping appears to be due to vertical cumulus scale transports which tend to balance the forcing by cumulus heating. In the western section of friction at 850 mb due to the mountainous region of the southern China coast provides the main damping mechanism in the mature stage. In the decaying stage the low-level trough moves southward offshore and weakens as a result of the decreasing baroclinic field, indicating that CISK cannot maintain the trough without the large-scale baroclinic forcing.

From the foregoing results the Mei-Yu trough appears to be a mixed midlatitude-tropical system. This trough is established when East Asian polar fronts repeatedly move southward into southeastern China and southern Japan during the pre- and early summer. The strong modification of the western segment of the front is in distinct contrast to the eastern segment, although cumulus convection and intense precipitation are important in the entire trough region. The present study is limited to one case only and is limited to the mature and decaying stages of the trough after the quasi-stationary position has already been established. Plans are now being made to study more cases and to include the developing stage which hopefully will shed more light on the development and physical mechanisms of the early summer monsoon trough in East Asia.

Acknowledgments. This work was supported by the National Science Foundation, Global Atmospheric Research Program, under Grant ATM77-14821 and U.S.-R.O.C. Cooperative Science Program, under Grant INT78-14557, and by the Naval Environmental Prediction Research Facility. We wish to thank Prof. R. T. Williams for discussions and Prof. R. L. Haney for reading the manuscript. One of us (TJC) wishes to thank the R.O.C. National Science Council for sponsoring in part his sabbatical leave from National Taiwan University.

REFERENCES

Akiyama, T., 1973: Ageostrophic low-level jet stream in the Baiu season associated with heavy rainfalls over the sea area. *J. Meteor. Soc. Japan,* **51,** 205–208.

——, 1974: mesoscale organization of cumulus convection in the large-scale rainband in the Baiu season. *J. Meteor. Soc. Japan,* **52,** 448–451.

Bosart, L. F., 1970: Mid-tropospheric frontogenesis. *Quart. J. Roy. Meteor. Soc.*, **96**, 442–471.

Chen, G. T. J., and L. F. Bosart, 1979: A quasi-Lagrangian vorticity budget of composite cyclone-anticyclone couplets accompanying North American polar air outbreaks. *J. Atmos. Sci.*, **36**, 185–194.

——, and C. Y. Tsay, 1977: A detailed analysis of a case of Mei-Yu system in the vicinity of Taiwan. Tech. Rep. Mei-Yu-001, Dept. Atmos. Sci., National Taiwan University, 249 pp.

——, and ——, 1978: A synoptic case study of Mei-Yu near Taiwan. *Pap. Meteor. Res.*, **1**, 25–36.

Matsumoto, S., 1972: Unbalanced low-level jet and solenoidal circulation associated with heavy rainfalls. *J. Meteor. Soc. Japan*, **50**, 194–203.

——, K. Ninomiya and S. Yoshizumi, 1971: Characteristic features of "Baiu" front associated with heavy rainfall. *J. Meteor. Soc. Japan*, **49**, 267–281.

Ninomiya, K., and T. Akiyama, 1971: The development of the medium-scale disturbances in the Baiu front. *J. Meteor. Soc. Japan*, **49**, 663–677.

——, and ——, 1972: Medium-scale echo clusters in the Baiu front as revealed by multi-radar composite echo maps. (Part I). *J. Meteor. Soc. Japan*, **50**, 558–569.

Reed, R. J., and R. H. Johnson, 1974: The vorticity budget of synoptic-scale wave disturbances in the tropical western Pacific. *J. Atmos. Sci.*, **31**, 1784–1790.

Wallace, J. M., 1971: Spectral studies of tropospheric wave disturbances in the tropical western Pacific. *Rev. Geophys. Space Phys.*, **9**, 557–612.